PHARMACIA

Pharmacia 69(1): 113–123
DOI 10.3897/pharmacia.69.e79467

Research Article

# Potential of hydroxybenzoic acids from *Graptopetalum paraguayense* for inhibiting of herpes simplex virus DNA polymerase – metabolome profiling, molecular docking and quantum-chemical analysis

Nadezhda Todorova[1], Miroslav Rangelov[2], Ivayla Dincheva[3], Ilian Badjakov[3], Venelin Enchev[4], Nadezhda Markova[2]

1 *Institute of Biodiversity and Ecosystem Research, Bulgarian Academy of Sciences, 1113 Sofia, Bulgaria*
2 *Institute of Organic Chemistry with Centre of Phytochemistry, Bulgarian Academy of Sciences, 1113 Sofia, Bulgaria*
3 *Department of Agrobiotechnologies, Agrobioinstitute, Agricultural Academy, 1164 Sofia, Bulgaria*
4 *Institute of General and Inorganic Chemistry, Bulgarian Academy of Sciences, 1113 Sofia, Bulgaria*

Corresponding author: Nadezhda Markova (nadya@orgchm.bas.bg)

**Received** 16 December 2021 ♦ **Accepted** 20 December 2021 ♦ **Published** 21 January 2022

**Citation:** Todorova N, Rangelov M, Dincheva I, Badjakov I, Enchev V, Markova N (2022) Potential of hydroxybenzoic acids from *Graptopetalum paraguayense* for inhibiting of herpes simplex virus DNA polymerase – metabolome profiling, molecular docking and quantum-chemical analysis. Pharmacia 69(1): 113–123. https://doi.org/10.3897/pharmacia.69.e79467

## Abstract

According to our previous investigation the total methanol extract from *Graptopetalum paraguayense* E. Walther demonstrates a significant inhibitory effect on herpes simplex virus type 1 (HSV-1). To clarify what causes this inhibitory activity on HSV-1, a metabolic profile of the plant was performed. Three main fractions: non-polar substances, polar metabolites and phenolic compounds were obtained and gas chromatography–mass spectrometry (GC-MS) analysis was carried out. Since it is well known that phenolic compounds show a significant anti-herpes effect and that viral DNA polymerase (DNApol) appears to play a key role in HSV virus replication, we present a docking and quantum-chemical analysis of the binding of these compounds to viral DNApol amino acids. Fourteen different phenolic acids found by GC-MS analyses, were used in molecular docking simulations. According to the interaction energies of all fourteen ligands in the DNApol pockets based on docking results, density functional theory (DFT) calculations were performed on the five optimally interacting with the receptor acids. It was found that hydroxybenzoic acids from phenolic fraction of *Graptopetalum paraguayense* E. Walther show a good binding affinity to the amino acids from the active site of the HSV DNApol, but significantly lower than that of acyclovir. The mode of action on virus replication of acyclovir (by DNApol) is different from that of the plant phenolic acids one, probably.

## Keywords

*Graptopetalum paraguayense* E. Walter, anti-HSV activities, hydroxybenzoic (phenolic) acids, molecular docking, DFT

## Introduction

Herpes simplex virus types 1 and 2 (HSV-1 and HSV-2) are members of the *Herpesviridae* family and are among the most common human pathogens, infecting about 90% of the world population (Boppana and Fowler 2007). Generally speaking, the main treatments available include several selective drugs that are classified as virucidal, immunomodulators, and chemotherapeutic agents. Common therapies for herpes infections employ nucleoside analogs, such as acyclovir (ACV), and target the viral DNA polymerase (DNApol), essential for viral DNA replication. However, the widespread use of such drugs has led to undesirable side effects and drug-resistant strains (Denaro and Smeriglio 2020). A better understanding of the herpes virus replication will help the development of new safe and effective broad-spectrum anti-herpetic drugs that fill an unmet need.

When searching for potent bioactive compounds, it is especially important to understand the nature of the interaction between biological macromolecules (enzymes, receptors) and small ligands (inhibitors, drugs). Theoretical chemistry can be used for the prediction of chemical structures and reactions, which would support biological testing, save time and resources. A promising way is to combine the complete three-dimensional structure of the biomacromolecule-ligand complex with theoretical energy calculations (Naray-Szabo 1984). A very important methodology for elucidating the reaction mechanisms and other properties of enzymes is the so-called quantum chemical cluster: a small part of the enzyme around the active site is treated with relatively accurate quantum chemical methods (Himo 2017). Quantum-chemical calculations, most commonly density functional theory (DFT), are increasingly crucial in computational enzymology.

The first studies on the antiviral activity of plant extracts were carried out in 1995–1996, and since then, researchers have made great strides in finding new plant sources of antiviral compounds. Plants are a rich and growing source of natural target molecules with different chemical structures that exhibit antiviral activity. Bioactive compounds are an important component in various extracts with potential anti-HSV activities. Crude extracts obtained from plants by various extraction methods have shown a wide spectrum of antiviral activity, including anti-HSV activity. A decisive factor for the ultimate success of the study of bioactive plant ingredients is the correct selection of plant materials and the appropriate process of extraction and purification of the active compounds. The main phytochemical substances that possess antiviral effects against HSV-1 and HSV-2 could be included in the following groups: alkaloids and nitrogenated compounds, coumarins, flavonoids, lignans, miscellaneous compounds, monoterpenoids, diterpenoids and sesquiterpenoids, phenolic acids, phenylpropanoids, quinones, tannins, thiophenes, triterpenoids and polyacetylenes (Perez 2003; Hassan et al. 2015; Treml et al. 2020). Phenolic compounds attract great interest due to their antioxidant activity and beneficial effects on human health (Saxena et al. 2012). Results from preliminary antiviral plate assay of the green solvent (hydro-ethanolic) shoot extract of *Limonium densiflorum* showed that gallic acid and epigallocatechin gallate have strong activity, while pinoresinol and *N-trans*-ferulolyl tyramine have moderate activity (Medini et al. 2016). It was found that phenolic compounds from acetonic and methanolic extract of apple pomace inhibit both HSV-1 and HSV-2 replication in Vero cells by more than 50%, at non-cytotoxic concentrations (Suárez et al. 2010).

Viral replication is not the only therapeutic goal studied, as several in vitro studies have shown that many plant extracts (eg aqueous root and bark extract of *Rhus aromatica* L. (Reichling et al. 2009) as well as aqueous and hydroalcoholic extracts of propolis (Nolkemper et al. 2010)) and their isolated compounds can inhibit the penetration of a virus. The authors attribute the anti-herpetic activity to the interference of the extracts with the viral envelope structures required for adsorption. Phenyl carboxylic acids, as well as polyphenols, have been identified as responsible compounds, although the synergistic activity of the plant complex has been suggested.

*Graptopetalum paraguayense* E. Walther (GP) is a species of succulent plant that belongs to the jade family *Crassulaceae*, originating from Tamaulipas, Mexico. In Taiwan, *Graptopetalum paraguayense* is a medicinal plant that is considered a vegetable with health benefits. As early as ancient China GP was traditionally used to treat a number of diseases: modulating blood pressure, relieving liver disease, relieving pain and infections, detoxification. Reported biological effects of GP include tyrosinase inhibition (Huang et al. 2005), antioxidants (Chao et al. 2019), regulation of hypertension (Chen et al. 2007; Chung et al. 2009), hepatoprotective effect (Duh et al. 2011; Hsu et al. 2019), antitumor activity (Ai et al. 2017), anti-inflammatory (Chen et al. 2016) and Alzheimer's disease therapy (Wu et al. 2019). There are no data in the literature on the antiviral activity (including anti-herpes activity) of GP. Recently we found that the total methanol extract from the plant demonstrates a significant inhibitory effect on HSV-1 (Zaharieva et al. 2019). Therefore, it is important to investigate the metabolic profile of the plant and which metabolites are responsible for this activity. Since virus-encoded DNA polymerase appears to be a key feature in the replication of large DNA viruses such as HSV, we present metabolome analysis of the plant *Graptopetalum paraguayense* E. Walther as well as theoretical investigations on the binding expedient of the compounds from phenolic fraction to viral DNA polymerase amino acids.

## Materials and methods

### Plant material and GP extracts preparation

#### *Plant material*

*G. paraguayense* E. Walter was grown as an ornamental plant at the Institute of Organic Chemistry with Centre of

Phytochemistry, Sofia, Bulgaria. Botanical identification and authentication were performed by Asen Asenov PhD (Sofia University 'St. Kliment Ohridski') and Antoaneta Petrova PhD (Botanical Garden, Bulgarian Academy of Sciences), and a voucher specimen number SO 107 621 was deposited in the herbarium of Sofia University, Bulgaria.

### Chemicals

Methanol, chloroform,, sulphuric acid, hydrochloric acid, ethyl acetate, n-hexane, pyridine were HPLC grade (Sigma-Aldrich, St. Louis, MO), mixture of aliphatic hydrocarbons (C8-C40) (Sigma). Sodium hydroxide, methoxyamine hydrochloride, N,OBis(trimethylsilyl)trifluoroacetamide (BSTFA), nonadecanoic acid methyl ester, ribitol and 35-dichloro-4-methoxybenzoic acid were purchased from Sigma-Aldrich, St. Louis, MO and water was of Milli-Q (18 MΩ/cm) (Millipore Corp., Bedford, MA).

### Extract preparation

Leaf extract was prepared as described in our previous study (Zaharieva et al. 2019). Briefly, 1.0 g of the freeze-dried material was mixed with 20.0 mL a methanol/water (75:25, v/v) solution and 50.0 µL of each internal standard (nonadecanoic acid methyl ester, ribitol, and 3-5-dichloro-4-methoxybenzoic acid, each in concentration 10.0 mg/mL for the quantification of metabolites of fractions A, B, and C, respectively), followed by heating at 70 °C for 1 h in a laboratory thermo mixer (Analytik Jena AG). The solution, cooling to room temperature was subjected to the following procedure: 8.0 mL chloroform and 2.0 mL water were added, then the mixture was centrifuged (5 min/22 °C/13000 rpm). The lower phase "A" was designed for the analysis of non-polar substances. The upper phase was divided into two equal parts (the first one "B" – for the study of the polar metabolites and the second one "C" – for the phenolic compounds). The three phases obtained were vacuum-dried in a centrifugal vacuum concentrator (Labconco Centrivap) at 40 °C. To the dried residue of fraction "A" 1.0 mL 2% $H_2SO_4$ in methanol were added and the mixture was heated on Thermo-Shaker TS100 (1 h/96 °C/300 rpm). After cooling, the solution was extracted with n-hexane (3×10.0 mL). Combined organic layers were vacuum-dried in a centrifugal vacuum concentrator (Labconco Centrivap) at 40 °C.

Fraction "C" was further processed. To the dried residue, 10.0 mL 1M NaOH (SigmaAldrich, MO) were added and the solution was kept overnight (12 h) at room temperature, then the pH was adjusted to 2 with 1M HCl and the mixture was heated on Thermo-Shaker TS-100 (1 h/96 °C/300 rpm). After cooling, the solution was extracted with ethyl acetate (3×10.0 mL). Combined organic layers were vacuum-dried in a centrifugal vacuum concentrator (Labconco Centrivap) at 40 °C. Fractions "A", "B" and "C" were subjected to further analyses.

### GC-MS sample preparation

Prior to the gas chromatography–mass spectrometry (GC-MS) analysis, fractions "A", "B" and "C" were derivatized by the following procedures. 100.0 µL pyridine and 100.0 µL BSTFA were added to the dried residues (fractions "A" and "C"), then heated on Thermoshaker, Analytik Jena AG, Germany (45 min/70 °C/300 rpm). 1.0 µL from the solution was injected into the GC-MS.

300.0 µL solution of methoxyamine hydrochloride (20.0 mg/mL in pyridine) was added to 5.0 mg fraction "B", and the mixture was heated on Thermo-Shaker TS-100 (1 h/70 °C/300 rpm). After cooling, 100.0 µL BSTFA were added to the mixture then heated on Thermoshaker, Analytik Jena AG, Germany (40 min/70 °C/300 rpm). 1.0 µL from the solution was injected into the GC-MS system.

### GC-MS

GC-MS analysis was carried out on a 7890A gas chromatograph (Agilent Technologies) interfaced with a 5975C mass selective detector (Agilent Technologies). Separations were performed using a 30 m × 0.25 mm (i.d.) DB-5 ms silica-fused capillary column coated with 0.25 µm film of poly (dimethylsiloxane) as the stationary phase. The flow rate of the carrier gas (helium) was maintained at 1.0 ml/min. The injector and the transfer line temperature were kept at 250 °C. The oven temperature program used was: 100 °C for 2 min then 15 °C/min to 180 °C for 1 min then 5 °C/min to 300 °C for 10 min. The injections were carried out in a split mode (10:1). The mass spectrometer was scanned from 50 to 550 m/z. All mass spectra were acquired in electron impact (EI) mode with 70 eV.

A mixture of aliphatic hydrocarbons (C8-C40) (Sigma) was injected into the system under the above temperature program in order to calculate the retention index RI (as Kovàts index) of each compound. Identification of compounds was obtained by comparing the RI and the spectral data from the Golm Metabolome Database (http://csbdb.mpimpgolm.mpg.de/csbdb/gmd/gmd.html) and NIST'08 (National Institute of Standards and Technology, USA).

## Computational details

### Molecular docking analysis

Fourteen different phenolic acids such as gallic, *trans*-ferulic, syringic acids, and others found by GS-MS analyses, were used in molecular docking simulations. For our model, we used the structure with PDB number 2GV9, which is a structure of the Herpes Simplex virus type 1 DNA polymerase, obtained by XRD with an overall resolution of 2.68 Å (Liu et al. 2006). The crystal structure was a dimer and for further work, we selected the B chain as it has fewer missing amino acids. The protein structure was prepared for docking according to the implemented structure preparation algorithm in MOE software (Group CC 2020) and was protonated according to the implemented Protonate3D algorithm. The resultant structure was relaxed by rough steepest descent optimization with MMFF94 force field and Born solvation water model. The site finder algorithm (Group CC 2020) was used to identify sites for the docking procedure and two of them, that

lie on the contact surface between protein and DNA and are close to amino acids in active site of the DNA polymerase, were selected for further work. Conformation library for the docking study was generated using LowModeMD methodology with MMFF94 force field and energy window for collection of conformations 50 kcal $mol^{-1}$ from the lowest energy conformation. All conformations of all ligands were docked in the two selected pockets using Triangle Matcher algorithm for the initial placement of every structure, which returns up to 10 000 000 poses of every ligand inside a pocket.

These poses were scored by London ΔG (Group CC 2020) function, which estimates the free energy of binding of the ligand from a given pose and consists of terms that weigh up average gain/loss of rotational and translational entropy and loss of flexibility of the ligand, measures geometric imperfections of hydrogen bonds and desolvation energy of atoms.

The best 50 poses for every ligand for every pocket were further optimized with Induced Fit methodology using MMFF94 force field and optimization cutoff of 6A from the ligand (Naïm et al. 2007). The GBVI/WSA ΔG (Group CC 2020) was used as a rescoring function and the best 30 poses were collected for the next coming analysis.

### *Quantum-chemical calculations*

According to the interaction energies of all fourteen ligands (phenolic acids from fraction "C") in the pockets based on the GBVI/WSA ΔG scoring function, DFT calculations were performed on the five optimally interacting with the receptor acids. The B3LYP (Lee et al. 1988; Becke 1993) functional has been widely used over the years as it has been found to provide a good balance between speed and accuracy. Thus, geometric optimization of the hydroxybenzoic acids *trans*-ferulic, gallic, syringic, vanillic, gentisic acids, and acyclovir, as well as amino acids from DNA polymerase active site and the complexes of the phenolic acids (and acyclovir) with amino acids, was carried out at B3LYP/6-31+G(d,p) computational level without symmetry constraints. Hydroxybenzoic acids and some of the amino acids that interact in the active center pocket of the enzyme are deprotonated. The same applies to acyclovir and its interacting amino acids. Acyclovir as an inhibitor of viral DNA synthesis is monophosphorylated by virus-encoded thymidine kinase (TK). Subsequent diphosphorylation and triphosphorylation are catalyzed by host cell enzymes, resulting in acyclovir triphosphate (Kimberlin 2018). Therefore, we use in our model acyclovir triphosphate (deprotonated at the three hydroxyl groups) located in the active site of HSV DNA polymerase. The local minima were verified by establishing that the Hessians had zero eigenvalues. The values of Gibbs free energies (G298) were calculated for a temperature of 298.15 K. To simulate the medium influence, the structures of acyclovir triphosphate, phenolic and amino acids as well as their complexes, were optimized again in argon medium ($\varepsilon$ = 1.430) using solvation model density (SMD) of Truhlar and coworkers (Marenich et al. 2009) at the same computational level (SMD/B3LYP/6-31+G(d,p)). This is the recommended choice for computing ΔG of solvation and it has the advantage of being parameterized for more than 100 solvents. The dielectric constant of the medium (the pocket of the enzyme site surrounding the phenolic acid and acyclovir complexes) was set to 1 and we chose the argon as medium to mimic the nature of the enzyme inside based on the previous studies (Foley et al. 2010; Ceña-Diez et al. 2016). The nature of the local minima on the potential energy surface was checked again by the absence of imaginary frequency. The DFT calculations were performed using Gaussian09 software package (Frisch et al. 2009).

## Results and discussion

In our pilot study (Zaharieva et al. 2019) on the anti-herpes activity of *Graptopetalum paraguayense* E. Walther (Fig. 1), we showed that the total GP methanol extract demonstrated a significant inhibitory effect on HSV-1 (97.5% cell protection), compared to ACV (with total protection of the cells 100%). The in vitro cytotoxicity assays of the GP extract indicate that it is characterized by a high cell tolerable concentration range. The results showed that the GP extract could be administrated in a concentration range (maximal nontoxic concentration, MNC, and lower) that avoids significant cell damage. The present study aims to further clarify both the organic composition of the plant and the mechanism of action of its main phytochemical components.

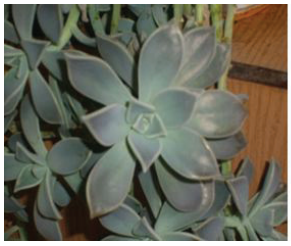


**Figure 1.** *Graptopetalum paraguayense* E. Walther.

The GC-MS analysis of the polar fraction enables qualitative and quantitative determination of *Graptopetalum paraguayense* E. Walther components present in the studied sample. A total of 33 compounds belonging to different chemical classes, mainly amino and organic acids, sugar alcohols, mono- and dicarbohydrates were established (Suppl. material 1: Table 1S). The predominant components in the essential amino acid class were leucine (92.04 μg/g DW), phenylalanine (82.72 μg/g DW) and isoleucine (80.74 μg/g DW), whereas in the non-essential amino acids class – tyrosine (37.75 μg/g DW), glycine (34.89 μg/g DW) and proline (33.28 μg/g DW), respectively. The major constituents in class of organic and inorganic acids were malic (1830.54 μg/g DW), citric (110.94 μg/g DW), and phosphoric acids (23.40 μg/g DW). The class of sugar alcohols was characterized by large amount of glycerol (329.58 μg/g DW) and myo-inositol (37.59 μg/g DW). The main components in

the class of monocarbohydrates were mannose (1335.38 μg/g DW) and sedoheptulose (803.77 μg/g DW), whereas in the class of dicarbohydrates – sucrose (473.52 μg/g DW).

The amount of phenolic components was 1701.50 μg/g DW (Table 1). The major components identified in this fraction were 1,8-dihydroxyanthraquinone (426.83 μg/g DW), followed by syringic acid (291.36 μg/g DW), *trans*-ferulic acid (218.97 μg/g DW), gallic acid (183.27 μg/g DW), and *p*-coumaric acid (147.80 μg/g DW), which represent 2/3 of the total phenolic compounds.

The main saturated fatty acids were palmitic (432.87 μg/g DW), stearic (122.24 μg/g DW) and behenic (119.56 μg/g DW) acids (Suppl. material 1: Table 2S). Linolenic (2842.50 μg/g DW), linoleic (2522.25 μg/g DW) and oleic (459.56 μg/g DW) acids represent 84% from the total lipid compounds.

**Table 1.** Phenolic components fraction from *G. paraguayense* determined by GC-MS analysis. DW – dried weight (μg/g), RT – retention time, RI – Kovàts retention indices, TMS – trimethylsilyl derivatives.

| Name | RT | $RI_{lit}$ | $RI_{calc}$ | DW |
|---|---|---|---|---|
| Salicylic acid (2TMS) | 8.01 | 1510.2 | 1510.3 | 41.57 |
| *m*-Hydroxybenzoic acid (2TMS) | 8.51 | 1576.9 | 1577.0 | 24.68 |
| 4-Hydroxyphenylethanol (2TMS) | 8.58 | 1580.6 | 1580.7 | 18.35 |
| *p*-Hydroxybenzoic acid (2TMS) | 9.19 | 1640.3 | 1640.4 | 20.32 |
| *p*-Hydroxyphenylacetic acid (2TMS) | 9.34 | 1665.8 | 1665.9 | 32.98 |
| Phloretic acid (2TMS) | 10.89 | 1763.2 | 1763.3 | 58.94 |
| Vanillic acid (2TMS) | 11.02 | 1776.0 | 1776.3 | 80.32 |
| Gentisic acid (3TMS) | 11.15 | 1788.8 | 1788.9 | 70.59 |
| Protocatechuic acid (3TMS) | 11.77 | 1813.3 | 1813.4 | 85.50 |
| Syringic acid (2TMS) | 12.92 | 1911.3 | 1911.4 | 291.36 |
| *p*-Coumaric acid (2TMS) | 13.48 | 1946.9 | 1947.0 | 147.80 |
| Gallic acid (4TMS) | 13.92 | 1969.0 | 1969.1 | 183.27 |
| *trans*-Ferulic acid (2TMS) | 15.90 | 2103.0 | 2103.1 | 218.97 |
| 1,8-Dihydroxyanthraquinone | 16.25 | 2125.5 | 2125.6 | 426.84 |
| Total phenolic compounds | | | | 1701.50 |

**DW** – dried weight (μg/g), **RT** – retention time, **RI** – Kovàts retention indices, **TMS** – trimethylsilyl derivatives.

Overall, *β*-amyrin (2080.86 μg/g DW), *β*-sitosterol (2010.41 μg/g DW), and *α*-tocopherol (1447.18 μg/g DW) were the predominant compounds in the fraction of sterols, terpenoids, and tocopherols (Suppl. material 1: Table 3S).

Because many of the hydroxybenzoic acids found in GP have shown a significant ability to inhibit HSV viral replication (Suárez et al. 2010; Medini et al. 2016; Yildirim et al. 2016; Hassan and Švajdlenka 2017; Chojnacka et al. 2021), our study was desined to all compounds. Fourteen different phenolic acids such as gallic, *trans*-ferulic, syringic acids, and others found by GS-MS analyses (Table 1) were used in molecular docking simulations. All docked structures were sorted according to their binding energy and the five best ligands according to ligand-pocket interactions were selected: *trans*-ferulic, gallic, syringic, vanillic and gentisic acids, as well as acyclovir triphosphate for comparison. *trans*-Ferulic acid, acyclovir triphosphate and their vicinity after docking procedure is shown in Figs 2 and 3 as an example. These five acids have the highest energy of interaction with the receptor and were used in further DFT calculations. Gallic, syringic, vanillic and gentisic ac-

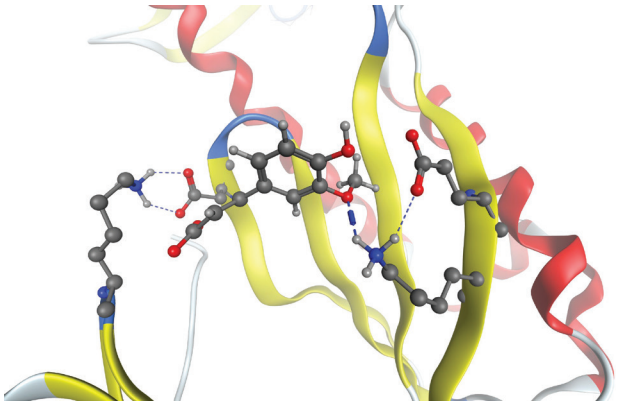

**Figure 2.** Phenolic (*trans*-ferulic) acid and its vicinity after docking procedure. The amino acid residues of HSV-1 DNA polymerase active site, mostly involved in interaction with ligands, are represented as follows: Lis928 is basic amino acid right from the ligand, Glu 927 is above it, basic amino acid on the left is Lis 939 and Asp 886 is in its right.

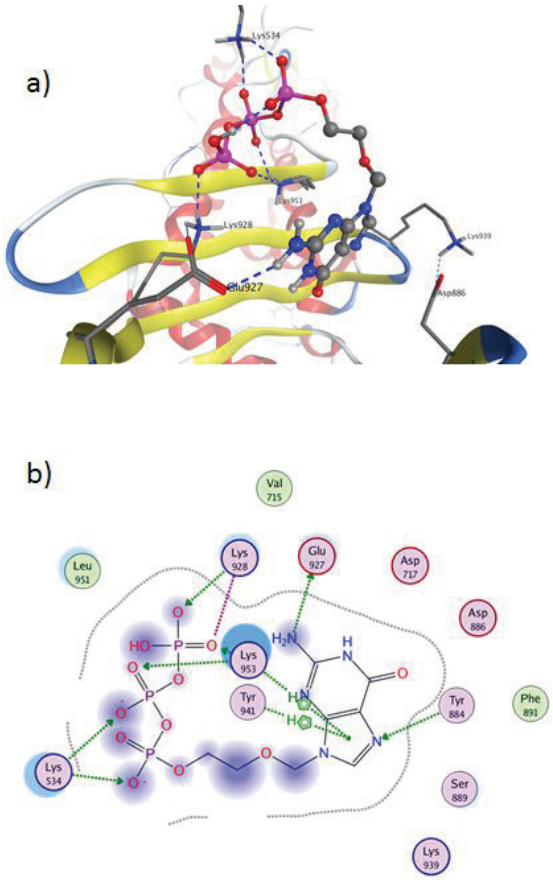


**Figure 3.** Acyclovir triphosphate and its vicinity in the DNA polymerase pocket after docking procedure: a) 3D plane of view and b) 2D plane of view. The interactions of the ligand in the active site cavity are represented as follows: the proximity contour is depicted with a black dotted line; solvent accessibility, as blue clouds around atoms or blue shadows around amino acid residues; polar amino acids are displayed with pink, while the lipophilic ones are in green. Basic amino acids are outlined with blue and the acidic – with red. Hydrogen bond interactions are depicted with dotted arrows, while the ionic ones are depicted with dotted lines.

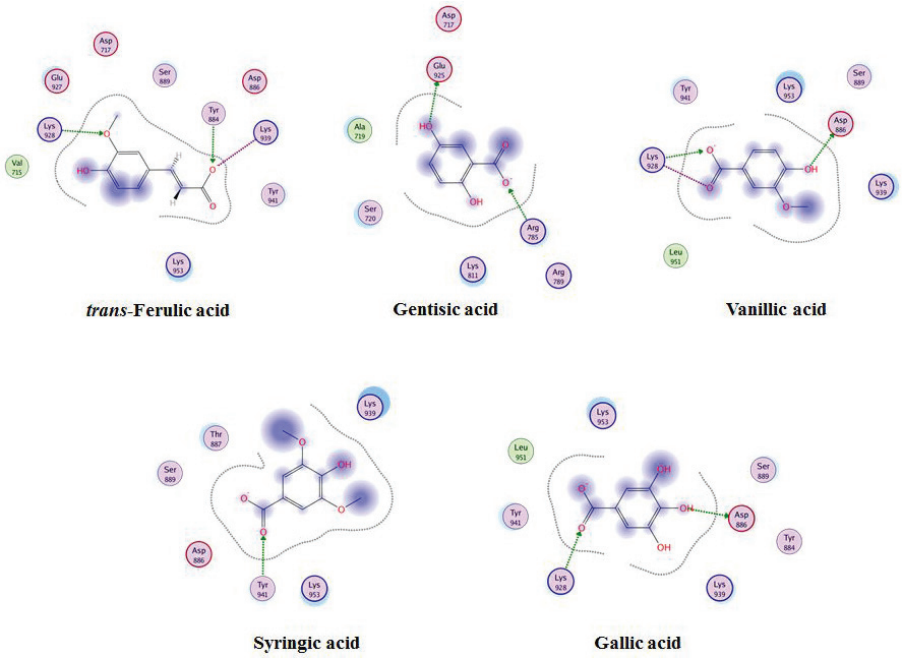


**Figure 4.** Fitting of phenolic acids in the DNA polymerase pocket.

ids and their vicinity after docking procedure are presented in Suppl. material 1: Figs S1–S4. As can be seen from the interaction maps in Figs 3 and 4, the main interaction energy terms are hydrogen bond interactions and ionic ones.

To clarify the affinity of *trans*-ferulic (*t*FA), gentisic (GntA), vanillic (VA), syringic (SA) and gallic acids (GA) (Fig. 5) conjugation to amino acids (AA) in DNA polymerase (Fig. 6), quantum-chemical calculations at B3LYP/6-31+G(d,p) level were performed based on molecular docking results. We started by modeling hydrogen-bonded complexes between the hydroxybenzoic acids, amino acids and two water molecules (Fig. 7). Thus, the complexes constructed show non-covalent interactions only qualitatively in the enzyme center, but could nevertheless provide indicative information on the inhibitory activity of phenolic acids from GP. The surroundings in the active enzyme pocket of phenolic acids (PA) were simulated as follows: *trans*-ferulic acid interacts with one molecule of protonated tyrosine (pTyr), two molecules lysine (Lys) and two water molecules (*t*Fa-Lys-pTyr-Lys-2$H_2O$).

GntA binds by hydrogen bonds to protonated arginine (pArg), glutamic acid (Glu) and two water molecules (GntA-Glu-pArg-2$H_2O$); vanillic acid conjugates with protonated lysine (pLys), aspartic acid (Asp) and two water molecules (VA-pLys-Asp-2$H_2O$); the binding of SA to pTyr and two water molecules leads to the formation of the hydrogen-bounded complex SA-pTyr-2$H_2O$; gallic acid interacts with pLys, Asp and two water molecules to form GALys-Asp-2$H_2O$ complex.

There are two possible sites of association of amino acids to PA by hydrogen bonding – to the carboxyl group (protonated amino acids) or to the hydroxyl groups (neutral amino acids). The protonated amino acid takes part in hydrogen bonding by –$NH_3^+$ group, while the neutral amino acid by =O (-OH) groups. The complexes formed between hydroxybenzoic acids and the corresponding amino acids are shown in Fig. 7.

To evaluate the binding expedient of PA to the corresponding AA of the enzyme active site and to compare it with a reference, quantum-chemical calculations on acyclovir triphosphate-amino acids complex were performed at the same theoretical level. This is necessary because the available treatments are based on several selective drugs such as acyclovir, which are able to inhibit DNA polymerase (Denaro and Smeriglio 2020). In this way, the inhibitory activity of phenolic acids from GP to viral DNApol could be compared with that of acyclovir triphosphate (AcvTP). The surroundings in the active enzyme pocket of AcvTP were simulated similarly to phenolic acids, according to molecular docking results. The three hydroxyl groups from the phosphate residue in the acyclovir triphosphate molecule are deprotonated and interact with three protonated lysine molecules (at amino groups) in the enzyme active site (Fig. 8). AcvTP binds by hydrogen bonds to Glu, Tyr and two water molecules forming AcvTP-3pLys-Glu-Tyr-2$H_2O$ complex.

All species (PA, AcvTP, AA and water molecules), as well as all complexes, were optimized at the B3LYP/6-31+G(d,p) level of theory.

In order to evaluate the possibility of intermolecular hydrogen bonds formation between PA and AA, the energies of interaction ($E_{int}$) and interaction free Gibbs energies ($G_{int}$) were calculated by eq. (1) and (2):

$$E_{int} = E_{PA} + E_{AA} + 2E_{water} - E_{complex} \quad (1)$$

$$G_{int} = G_{PA} + G_{AA} + 2G_{water} - G_{complex} \quad (2)$$

$E_{PA}$, $E_{AA}$, $E_{water}$, and $E_{complex}$ are the Et energies; $G_{PA}$, $G_{AA}$, $2G_{water}$, and $G_{complex}$ are the $G_{298}$ energies, calculated at B3LYP/6-31+G(d,p) level, for each phenolic acid, ami-

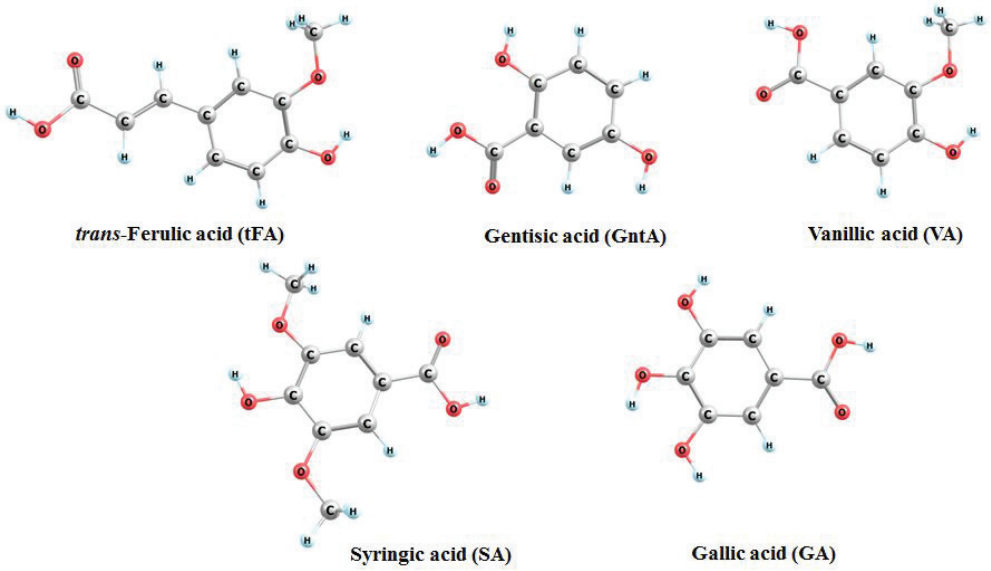


**Figure 5.** Structures of hydroxybenzoic acids from GP phenolic fraction "C", optimized at B3LYP/6-31+G(d,p) level.

no acids, AcvTP, water molecules and its complex, respectively. $E_{int}$ and $G_{298}$ of all complexes are presented in Table 2.

**Table 2.** Interaction energies, $E_{int}$, and interaction free Gibbs energies, $G_{int}$, (in kcal mol$^{1}$), for the complexes of the GP hydroxybenzoic acids and acyclovir triphosphate (as a referent) with DNA polymerase amino acids calculated at B3LYP/6-31+G(d,p) and SMD/B3LYP/6-31+G(d,p) levels.

| Complex type | $E_{int}$ | $G_{int}$ |
|---|---|---|
| *gas phase* | | |
| *t*Fa-Lys-pTyr-Lys-2$H_2O$ | 163.40 | 104.12 |
| GntA-Glu-pArg-2$H_2O$ | 163.63 | 119.89 |
| VA-pLys-Asp-2$H_2O$ | 157.61 | 112.54 |
| SA-pTyr-2$H_2O$ | 139.47 | 105.96 |
| GA-Lys-pAsp-2$H_2O$ | 155.93 | 110.10 |
| AcvTP-3pLys-Glu-Tyr-2$H_2O$ | 698.31 | 477.28 |
| *argon* | | |
| *t*Fa-Lys-Tyr-Lys-2$H_2O$ | 127.57 | 69.21 |
| GntA-Glu-Arg-2$H_2O$ | 125.27 | 79.03 |
| VA-Lys-Asp-2$H_2O$ | 119.93 | 76.36 |
| SA-Tyr-2$H_2O$ | 106.23 | 71.37 |
| GA-Lys-Asp-2$H_2O$ | 118.47 | 72.46 |
| AcvTP-3Lys-Glu-Tyr-2$H_2O$ | 422.04 | 327.06 |

When the calculations were performed in gas phase, the most stable complex is that of AcvTP: AcvTP-3Lys-Glu-Tyr-2$H_2O$. The interaction energy ($E_{int}$) is 698.31 kcal mol$^{-1}$. According to our results for all phenolic acids, the most stable complexes are formed with *t*FA and GntA. The values of $E_{int}$ are 163.40 and 163.63 kcal mol$^{-1}$, respectively. Next in the stability scale are the complexes of VA (157.61 kcal mol$^{-1}$) and GA (155.93 kcal mol$^{-1}$). As can be seen from the results received, the interaction energy of acyclovir triphosphate complex is more than four times higher than that of *t*FA and GntA complexes (with highest $E_{int}$). The reason could be in the larger number of deprotonated -OH groups in the AcvTP molecule than in the phenolic acids ones. This leads to stronger binding of AcvTP to the active site of the enzyme compared to PA from GP.

The picture is slightly different when the free Gibbs energies of interaction were considered: the AcvTP complex again has the highest interaction energy (477.28 kcal mol$^{-1}$), but the energy differences with hydroxybenzoic acids complexes decrease by an order of magnitude (Table 2). As can be seen from the table, all hydroxybenzoic acids complexes are close by free Gibbs interaction energy: between 104 and 119 kcal mol$^{-1}$.

When the SMD formalism at B3LYP/6-31+G(d,p) level was applied to account medium (argon) influence on the stability of the complexes formed, the energies of interaction $E_{int}$ decrease drastically: by 276.27 kcal mol$^{-1}$ for AcvTP complex and between 33–38 kcal mol$^{-1}$ for the five phenolic acids complexes. In this case, *t*Fa-Lys-pTyr-Lys-2$H_2O$ and GntA-GlupArg-2$H_2O$ again show the greatest affinity for hydrogen bonding to the DNApol active site, compared to the complexes of other phenolic acids: 127.57 and 125.27 kcal mol$^{-1}$, respectively. If we consider the complexes of AcvTP and phenolic acids as embedded in a solvation model density, the SMD/B3LYP/6-31+G(d,p) calculated free interaction energies ($G_{298}$) decrease also: by 150.22 kcal mol$^{-1}$ for AcvTP-3pLys-Glu-Tyr-2$H_2O$ and by 34–40 kcal mol$^{-1}$ for hydroxybenzoic acids complexes, relative to the gas-phase cluster.

As can be seen from the results presented, compounds from the phenolic fraction of GP show the good possibility for hydrogen binding to DNApol active site but significantly smaller than that of AcvTp. This could be due to two facts: i) Methods based on DFT provide treatment of the weak non-covalent interactions by false and irregular results. This is due to the fact that stabilization in these complexes is determined by dispersion interactions that are not accounted for by standard DFT functionalities (Rajchel et al. 2010); ii). Despite the good results for the binding expedient of the phenolic fraction of GP, it is likely that the mechanism of action of these compounds includes inhibition of HSV-1 replication not only through DNA polymerase but probably by other enzymes. It is possible that the manner of the inhibitory

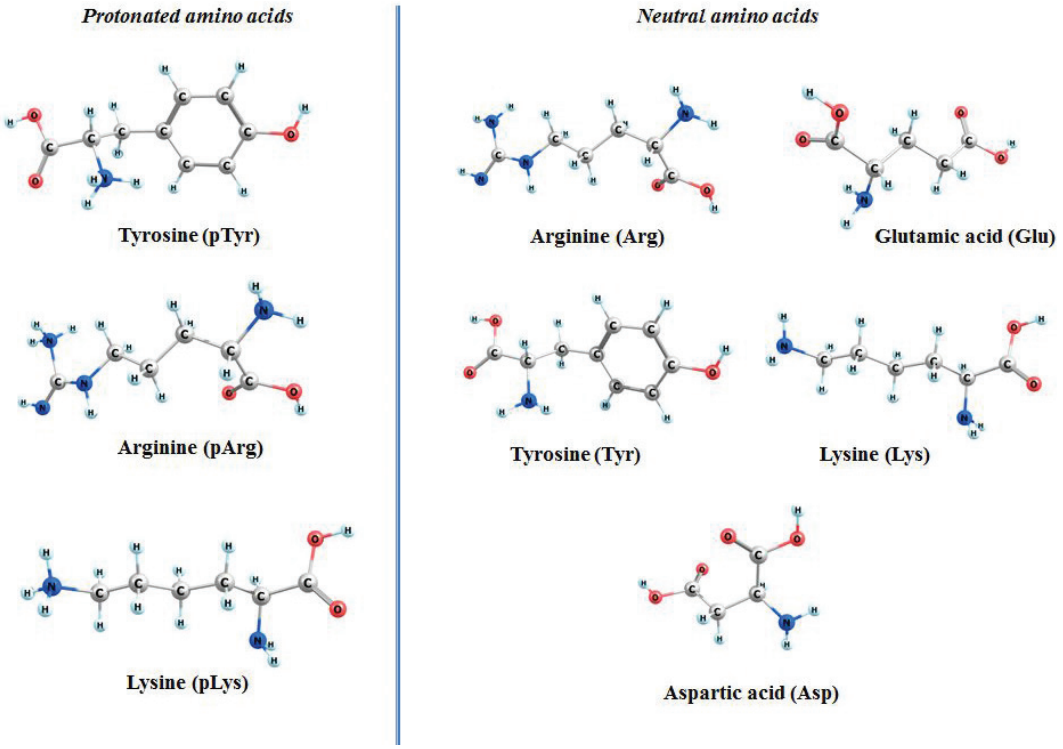


**Figure 6.** Structures of amino acids from GP phenolic fraction "C", optimized at B3LYP/6-31+G(d,p) level.

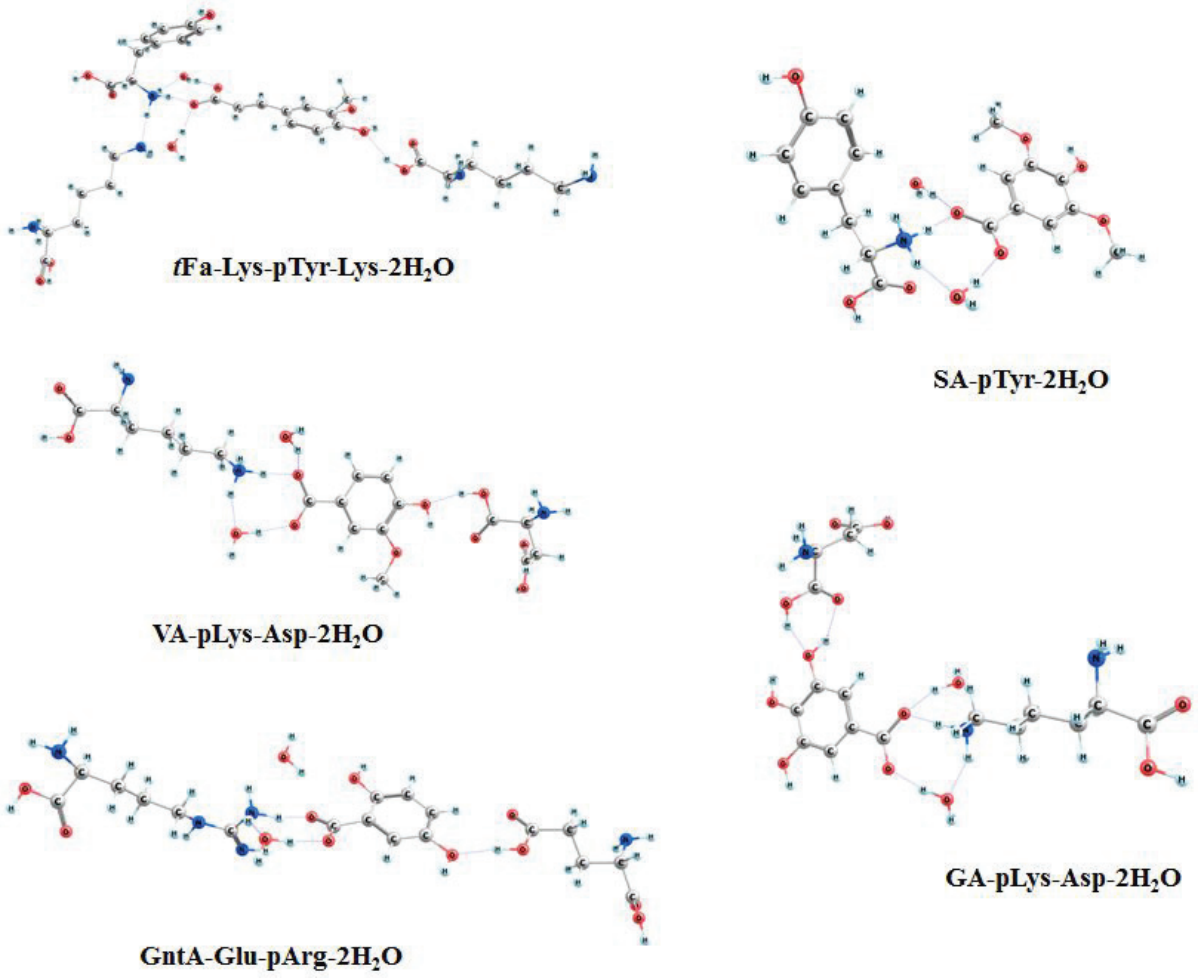


**Figure 7.** Complexes of phenolic acids from GP phenolic fraction "C" and amino acids from DNA polymerase active site, optimized at B3LYP/6-31+G(d,p) level.

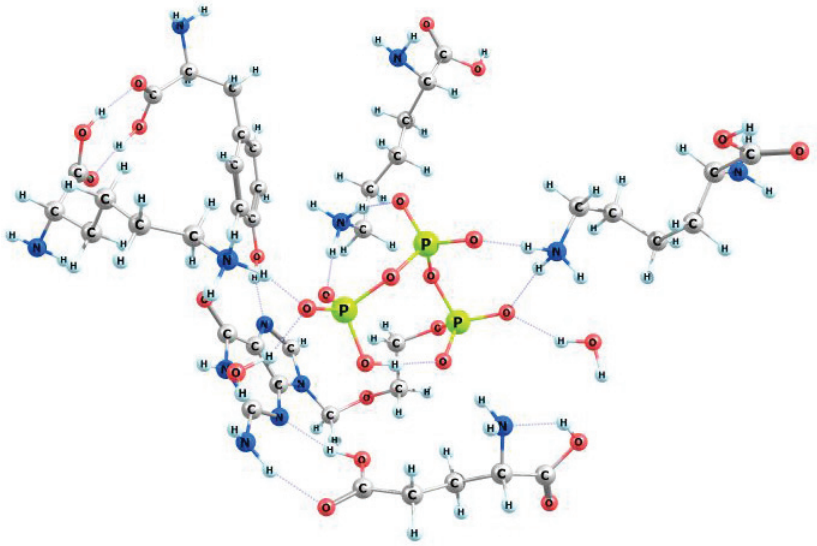


**Figure 8.** Complex of acyclovir triphosphate and amino acids from DNA polymerase active site, optimized at B3LYP/6-31+G(d,p) level.

activity on virus replication of AcvTP (by DNA polymerase) is different from that of the plant hydroxybenzoic acids one. Further investigations in this direction would help to clarify the antiviral activity of *Graptopetalum paraguayense* E. Walther.

## Conclusions

Current treatment for HSV infection relies mainly on the use of acyclovir and related synthetic nucleoside analogs. The widespread use of these drugs has led to the establishment of side effects and drug-resistant strains, which has increased the need for new natural antiviral agents. Total methanol extract from the succulent plant *Graptopetalum paraguayense* E. Walther demonstrates a significant inhibitory effect on HSV-1, according to our recent study (Zaharieva et al. 2019). In order to explain this strong antiviral activity, metabolic analysis of the plant was performed. Three main fractions: non-polar substances, polar metabolites, and phenolic compounds were obtained and GC-MS analysis was carried out. Fourteen different phenolic acids such as gallic, *trans*-ferulic, syringic acids, and others found by GS-MS analyses, were used in molecular docking simulations. The optimally interacting with the receptor amino acids were used for quantum-chemical calculations at B3LYP/6-31+G(d,p) computational level to establish the binding affinity of hydroxybenzoic acids from GP to HSV DNApol active site. According to the interaction energies of all five ligand-amino acid complexes, the hydrogen bonding in all of them is strong but significantly weaker than that in the acyclovir complex. The reason could be in DFT methods used as well as in the mechanism of antiviral effect. It is possible the mode of the inhibitory activity on the virus replication of AcvTP (by DNA polymerase) is different from that of the plant hydroxybenzoic acids one. Further investigations in this sense would help to clarify the antiviral activity of *Graptopetalum paraguayense* E. Walther.

## Author Contributions

Conceptualization and visualization, N.M.; methodology, N.M., I.D., I.B.; software, N.M., M.R., N.T.; validation, I.D., I.B.; formal analysis, I.D., I.B.; investigation, N.M., I.D., I.B., M.R., N.T.; data curation, N.M., V.E.; writing – original draft preparation, N.M..; writing – review and editing, N.M., V.E., I.D.; supervision, N.M., V.E.; project administration, N.M.; funding acquisition, N.M. All authors have read and agreed to the published version of the man-uscript.

## Acknowledgements

This work was supported by the Bulgarian National Science Fund under Grant DN19/16/2017.

## References

Ai L, Chung Y-C, Jeng K-CG, Lai PFH, Yeh S-C, Lee KC, Lin S-Y, Xia Y, Wang G, Cui SW (2017) Antioxidant hydrocolloids from herb *Graptopetalum paraguayense* leaves show anticolon cancer cells and anti-neuroinflammatory potentials. Food Hydrocolloids 73: 51–59. https://doi.org/10.1016/j.foodhyd.2017.06.027

Becke AD (1993) Density-functional thermochemistry. III. The role of exact exchange. The Journal of Chemical Physics 98: 5648–5652. https://doi.org/10.1063/1.464913

Boppana SB, Fowler KB (2007) Persistence in the population: epidemiology and transmisson. In: Arvin A, CampadelliFiume G, Mocarski

E et al. (Eds) Human Herpesviruses: Biology, Therapy, and Immunoprophylaxis, Cambridge University Press, Cambridge.

Ceña-Diez R, Vacas-Córdoba E, García-Broncano P, de la Mata FJ, Gómez R, Maly M, MuñozFernández M (2016) Prevention of vaginal and rectal herpes simplex virus type 2 transmission in mice: mechanism of antiviral action. International journal of nanomedicine 11: 2147–2162. https://doi.org/10.2147/IJN.S95301

Chao WW, Chen SJ, Peng HC, Liao JW (2019) Antioxidant Activity of *Graptopetalum paraguayense* E. Walther Leaf Extract Counteracts Oxidative Stress Induced by Ethanol and Carbon Tetrachloride Co-Induced Hepatotoxicity in Rats. Antioxidants (Basel, Switzerland) 8: 251–265. https://doi.org/10.3390/antiox8080251

Chen S-J, Yen C-H, Liu J-T, Tseng Y-F, Lin P-T (2016) Anti-inflammatory effect of water extracts of *Graptopetalum paraguayense* supplementation in subjects with metabolic syndrome: a preliminary study. Journal of the Science of Food and Agriculture 96: 1772–1776. https://doi.org/10.1002/jsfa.7284

Chen SJ, Chang CT, Chung YC, Chou ST (2007) Studies on the inhibitory effect of *Graptopetalum paraguayense* E. Walther extracts on the angiotensin converting enzyme. Food Chemistry 100: 1032–1036. https://doi.org/10.1016/j.foodchem.2005.10.053

Chojnacka K, Skrzypczak D, Izydorczyk G, Mikula K, Szopa D, Witek-Krowiak A (2021) Antiviral properties of polyphenols from plants. Foods 10: 2277. https://doi.org/10.3390/foods10102277

Chung Y-C, Chen S-J, Peng H-Y, Chou S-T (2009) Antihypertensive and antioxidant effects of the Graptopetalum paraguayense E. Walther extract in spontaneously hypertensive rats. Journal of the Science of Food and Agriculture 89: 2678–2686. https://doi.org/10.1002/jsfa.3774

Denaro M, Smeriglio A (2020) Antiviral activity of plants and their isolated bioactive compounds: An update. Phytotherapy Research: PTR 34: 742–768. https://doi.org/10.1002/ptr.6575

Duh P-D, Lin S-L, Wu S-C (2011) Hepatoprotection of Graptopetalum paraguayense E. Walther on CCl4-induced liver damage and inflammatio. Journal of Ethnopharmacology 134: 379–385. https://doi.org/10.1016/j.jep.2010.12.029

Foley MC, Padow VA, Schlick T (2010) DNA pol λ's extraordinary ability to stabilize misaligned DNA. Journal of the American Chemical Society 132: 13403–13416. https://doi.org/10.1021/ja1049687

Frisch MJ, Trucks GW, Schlegel HB, Scuseria GE, Robb MA, Cheeseman JR, Scalmani G, Barone V, Mennucci B, Petersson GA, Nakatsuji H, Caricato M, Li X, Hratchian HP, Izmaylov AF, Bloino J, Zheng G, Sonnenberg JL, Hada M, Ehara M, Toyota K, Fukuda R, Hasegawa J, Ishida M, Nakajima T, Honda Y, Kitao O, Nakai H, Vreven T, Montgomery JA, Jr., Peralta JE, Ogliaro F, Bearpark M, Heyd JJ, Brothers E, Kudin KN, Staroverov VN, Kobayashi R, Normand J, Raghavachari K, Rendell A, Burant JC, Iyengar SS, Tomasi J, Cossi M, Rega N, Millam JM, Klene M, Knox JE, Cross JB, Bakken V, Adamo C, Jaramillo J, Gomperts R, Stratmann RE, Yazyev O, Austin AJ, Cammi R, Pomelli C, Ochterski JW, Martin RL, Morokuma K, Zakrzewski VG, Voth GA, Salvador P, Dannenberg JJ, Dapprich S, Daniels AD, Farkas Ö, Foresman JB, Ortiz JV, Cioslowski J, Fox DJ (2009) Gaussian 09, Revision D.01, in Gaussian, Inc, Wallingford CT.

Group CC (2020) MOE – MOE Software package QC, Montreal, Canada.

Hassan STS, Švajdlenka E (2017) Biological evaluation and molecular docking of protocatechuic acid from *Hibiscus sabdariffa* L. as a potent urease inhibitor by an ESI-MS based method. Molecules 22: 1696. https://doi.org/10.3390/molecules22101696

Hassan STS, Masarčíková R, Berchová K (2015) Bioactive natural products with anti-herpes simplex virus properties. Journal of Pharmacy and Pharmacology 67: 1325–1336. https://doi.org/10.1111/jphp.12436

Himo F (2017) Recent Trends in Quantum Chemical Modeling of Enzymatic Reactions. Journal of the American Chemical Society 139: 6780–6786. https://doi.org/10.1021/jacs.7b02671

Hsu WH, Liao SC, Chyan YJ, Huang KW, Hsu SL, Chen YC, Siu ML, Chang CC, Chung YS, Huang CF (2019) *Graptopetalum paraguayense* Inhibits Liver Fibrosis by Blocking TGF-beta Signaling In Vivo and In Vitro. International Journal of Molecular Sciences 20: 2592. https://doi.org/10.3390/ijms20102592

Huang KF, Chen YW, Chang CT, Chou ST (2005) Studies on the inhibitory effect of *Graptopetalum paraguayense* E. Walther extracts on mushroom tyrosinase. Food Chemistry 89: 583–587. https://doi.org/10.1016/j.foodchem.2004.03.022

Kimberlin DW (2018) 295 – Antiviral Agents. In: Long SS, Prober CG, Fischer M (Eds) Principles and Practice of Pediatric Infectious Diseases (5th ed.), Elsevier, 1551–1567. https://doi.org/10.1016/B978-0-323-40181-4.00295-4

Lee CT, Wang WT, Pople RG (1988) Development of the Colle-Salvetti correlation-energy formula into a functional of the electron density. Physical Review B 37: 785–789. https://doi.org/10.1103/PhysRevB.37.785

Liu S, Knafels JD, Chang JS, Waszak GA, Baldwin ET, Deibel Jr MR, Thomsen DR, Homa FL, Wells PA, Tory MC, Poorman RA, Gao H, Qiu X, Seddon AP (2006) Crystal structure of the herpes simplex virus 1 DNA polymerase. The Journal of biological chemistry 281: 1819318200. https://doi.org/10.1074/jbc.M602414200

Marenich AV, Cramer CJ, Truhlar DG (2009) Universal solvation model based on solute electron density and on a continuum model of the solvent defined by the bulk dielectric constant and atomic surface tensions. Journal of Physical Chemistry B 113: 6378. https://doi.org/10.1021/jp810292n

Medini F, Megdiche W, Mshvildadze V, Pichette A, Legault J, St-Gelais A, Ksouri R (2016) Antiviral-guided fractionation and isolation of phenolic compounds from Limonium densiflorum hydroalcoholic extract. Comptes Rendus Chimie 19: 726–732. https://doi.org/10.1016/j.crci.2016.03.006

Naïm M, Bhat S, Rankin KN, Dennis S, Chowdhury SF, Siddiqi I, Drabik P, Sulea T, Bayly CI, Jakalian A, Purisima EO (2007) Solvated Interaction Energy (SIE) for Scoring Protein–Ligand Binding Affinities. 1. Exploring the Parameter Space. Journal of Chemical Information and Modeling 47: 122–133. https://doi.org/10.1021/ci600406v

Naray-Szabo G (1984) Quantum chemical calculation of the enzyme-ligand interaction energy for trypsin inhibition by benzamidines. Journal of the American Chemical Society 106: 4584–4589. https://doi.org/10.1021/ja00328a048

Nolkemper S, Reichling J, Sensch KH, Schnitzler P (2010) Mechanism of herpes simplex virus type 2 suppression by propolis extracts. Phytomedicine: international journal of phytotherapy and phytopharmacology 17: 132–138. https://doi.org/10.1016/j.phymed.2009.07.006

Perez RM (2003) Antiviral Activity of Compounds Isolated From Plants. Pharmaceutical biology 41: 107–157. https://doi.org/10.1076/phbi.41.2.107.14240

Rajchel Ł, Żuchowski PS, Hapka M, Modrzejewski M, Szczęśniak MM, Chałasiński G (2010) A density functional theory approach to non-covalent interactions via interacting monomer densities. Physical Chemistry Chemical Physics: PCCP 12: 14686–14692. https://doi.org/10.1039/c0cp00626b

Reichling J, Neuner A, Sharaf M, Harkenthal M, Schnitzler P (2009) Antiviral activity of *Rhus aromatica* (fragrant sumac) extract against two types of herpes simplex viruses in cell culture. Die Pharmazie 64: 538–541.

Saxena M, Saxena DJ, Pradhan DA (2012) Flavonoids and phenolic acids as antioxidants in plants and human health. International Journal of Pharmaceutical Sciences Review and Research 16: 130–134.

Suárez B, Álvarez ÁL, García YD, Barrio Gd, Lobo AP, Parra F (2010) Phenolic profiles, antioxidant activity and in vitro antiviral properties of apple pomace. Food Chemistry 120: 339342. https://doi.org/10.1016/j.foodchem.2009.09.073

Treml J, Gazdová M, Šmejkal K, Šudomová M, Kubatka P, Hassan STS (2020) Natural ProductsDerived Chemicals: Breaking Barriers to Novel Anti-HSV Drug Development. Viruses 12: 154. https://doi.org/10.3390/v12020154

Wu P-C, Fann M-J, Tran TT, Chen S-C, Devina T, Cheng IH-J, Lien C-C, Kao L-S, Wang S-J, Fuh JL, Tzeng T-T, Huang C-Y, Shiao Y-J, Wong Y-H (2019) Assessing the therapeutic potential of Graptopetalum paraguayense on Alzheimer's disease using patient iPSC-derived neurons. Scientific Reports 9: 19301. https://doi.org/10.1038/s41598-019-55614-9

Yildirim A, Duran GG, Duran N, Jenedi K, Bolgul BS, Miraloglu M, Muz M (2016) Antiviral activity of hatay propolis against replication of herpes simplex virus type 1 and type 2. Medical Science Monitor 22: 422–430. https://doi.org/10.12659/MSM.897282

Zaharieva MM, Genova-Kalou P, Dincheva I, Badjakov I, Krumova S, Enchev V, Najdenski H, Markova N (2019) Anti-Herpes Simplex virus and antibacterial activities of Graptopetalum paraguayense E. Walther leaf extract: a pilot study. Biotechnology & Biotechnological Equipment 33: 12511259. https://doi.org/10.1080/13102818.2019.1656108

## Supplementary material 1

### Tables S1–S3 and Figures S1–S4

Authors: Nadezhda Todorova, Miroslav Rangelov, Ivayla Dincheva, Ilian Badjakov, Venelin Enchev, Nadezhda Markova

Data type: docx. file

Explanation note: Table S1. Polar metabolites fraction from *Graptopetalum paraguayense* determined by GC-MS analysis. Table S2. Main saturated fatty acids fraction from *G. paraguayense* determined by GC-MS analysis. Table S3. Sterol fraction from *G. paraguayense* determined by GC-MS analysis. Figure S1. Gallic acid and its vicinity after docking procedure. Figure S2. Gentisic acid and its vicinity after docking procedure. Figure S3. Syringic acid and its vicinity after docking procedure. Figure S4. Vanillic acid and its vicinity after docking procedure.



Link: https://doi.org/10.3897/pharmacia.69.e79467.suppl1